JOURNAL OF
POWER
SOURCES

Short communication

# Sol–gel processing of $Sr_{0.5}Sm_{0.5}CoO_3$ film

Zhaolin Tang[*], Yongsong Xie, Howard Hawthorne, Dave Ghosh

*Institute for Fuel Cell Innovation, National Research Council Canada, 3250 East Mall, Vancouver, BC V6T 1W5, Canada*

## Abstract

Strontium-doped samarium cobaltite ($Sm_{0.5}Sr_{0.5}CoO_3$, SSC) has attracted increasing attention as cathode material for intermediate-temperature solid oxide fuel cells (IT-SOFCs) due to its mixed-conduction characteristics and relatively high ionic conductivity. In this paper, sol–gel-derived SSC films were deposited on yttria stabilized zirconia (YSZ) substrates from an alkoxide solution of strontium isopropoxide, samarium isopropoxide and cobalt isopropoxide. The alkoxide solution was chelated with 2-ethylacetoacetate ($CH_3COCH_2COOC_2H_5$), and the effect of polyethylene glycol (PEG) addition on the crystallization behavior and microstructure evolution of SSC films was investigated. XRD, TGA and SEM measurements indicated that single-perovskite phase SSC films were formed when the films were heated at 700 °C, and PEG could significantly refine the crystalline size of the SSC film from around 100–50 nm.
© 2005 Elsevier B.V. All rights reserved.

*Keywords:* Solid oxide fuel cell; Cathode; Sol–gel processing; $Sm_{0.5}Sr_{0.5}CoO_3$

## 1. Introduction

Solid oxide fuel cells (SOFCs) are energy conversion devices, which have gained increasing interest in recent decades due to their high efficiency and low emission of pollutants [1,2]. While existing SOFC technology has demonstrated much higher energy efficiency, the cost of current SOFC systems is still prohibitive for broad commercialization except for demonstration plants. One effective approach to cost reduction is to reduce the operating temperature, for example, below 700 °C [3–5]. At such low operating temperature, the interconnect, heat exchange and structure components may be fabricated from relatively inexpensive metal components [6,7]. The lower operating temperature would also solve various problems associated with the higher temperature operation, such as densification of electrodes, formation of an insulating layer at the electrode/electrolyte interface by interdiffusion, and crack formation from stress caused by large differences in the thermal expansion coefficients of the cell components [4]. Reduction of operating temperature can be achieved either by thinning the electrolyte layer, or by using highly conductive electrolytes, such as doped ceria. At reduced operating temperatures, the cathode becomes critical for the fuel cell performance since the activation energy for cathodic reaction is very large [3,4].

Currently, $La_{1-x}Sr_xMnO_3$ perovskite (LSM) is commonly used as cathode material for SOFCs because of its high catalytic activity for oxygen reduction and thermal and chemical compatibility with yttria stabilized zirconia (YSZ) [1,8]. While LSM has shown promising performance for SOFCs operating at temperatures around 800 °C, its performance decreases rapidly as the operating temperature decreases. Therefore, considerable research interest is currently directed towards cobalt-containing perovskite oxides, which tend to exhibit mixed-conduction characteristics and relatively higher ionic conductivities than LSM due to a greater concentration of oxygen vacancies [9–11]. In particular, interest has grown in the strontium-doped samarium cobaltite with a composition of $Sm_{0.5}Sr_{0.5}CoO_3$ (SSC), which shows a high conductivity up to $10^3$ S cm$^{-1}$ [12]. It was also reported that the over potentials of SOFC cathodes made of SSC are low, and SSC shows good compatibility with ceria electrolyte [13].

* Corresponding author. Tel.: +1 604 221 3000; fax: +1 604 221 3088.
E-mail address: Zhaolin.tang@nrc.gc.ca (Z. Tang).

The electrochemical properties of cathodes depend not only on their chemical composition but also on their microstructure. The cathode microstructure is mostly related to the deposition process applied. Screen-printing is typically used to apply the electrode material on YSZ electrolytes. The screen-printed electrode is often fired above 1100 °C to assure strong contact with the electrolyte. Such a high temperature heat-treatment cannot only produces insulating phases, like $La_2Zr_2O_7$ or $SrZrO_3$ [14,15] but also reduces the surface area of the electrode, thus reducing its catalytic activity. Therefore, alternative processes, such as electroless plating, sol–gel processing, chemical vapor deposition, plasma processing and laser ablation have been proposed to improve the contact between the electrode and electrolyte, while retaining its porous microstructure [16,17]. Among the above methods, the sol–gel process provides several advantages: (i) the microstructure and composition of electrode materials can be controlled with relative ease, (ii) low-temperature processing is possible and (iii) the electrode and electrolyte adherence is strong. Currently, there are some reports related to the sol–gel processing of doped $LaMnO_3$ [18,19], but none on SSC. In the present study, SSC gelled films were prepared by dip-coating from the alkoxide precursor solution modified with an organic polymer (polyethylene glycol (PEG)), and the effects of PEG addition on crystallization behavior and microstructure evolution were investigated.

## 2. Experimental procedure

Strontium isopropoxide ($Sr(O-i-C_3H_7)_2$), samarium isopropoxide ($Sm(O-i-C_3H_7)_3$), and cobalt isopropoxide ($Co(O-i-C_3H_7)_2$) were used as starting materials (all chemicals were purchased from Alfa Aesar). First, 0.01 mol $Sr(O-i-C_3H_7)_2$ and 0.01 mol $Sm(O-i-C_3H_7)_3$) were completely dissolved with 250 ml 2-methoxyethanol ($CH_3OCH_2CH_2OH$) by stirring the solution at room temperature for 30 min. Subsequently, 0.02 mol $Co(O-i-C_3H_7)_2$ was added into this solution, and the solution was heated at 60 °C for 1 h. To increase the solubility of each alkoxide, and also to improve the stability of the alkoxide solution, 0.02 mol of a chelating agent, 2-ethylacetoacetate, ($CH_3COCH_2COOC_2H_5$), was added to the alkoxide solution. The solution was mixed and refluxed at 75 °C for 2 h in dried air. After cooling, 0.04 ml $H_2O$ diluted with 2-methoxyethanol (1.8 g) was added to the solution for partial hydrolysis and condensation. The molar ratio of $H_2O$ to the alkoxide ($H_2O:(Sm + Sr + Co)$) was 1. Half of the solution was taken out and modified with 4 g PEG ($HOCH_2(CH_2O·CH_2)_nCH_2OH$, mw = 2000). Both PEG modified and unmodified precursor solutions were stirred at room temperature for 2 h.

SSC thin films were deposited on polished YSZ substrate (1 cm × 2 cm) by dip-coating. Film deposition was carried out with a holding time of 30 s in the sol and a withdrawal speed of 7.6 cm min⁻¹. Subsequently, the samples were dried

at 80 °C for 10 min, and fired at 500–700 °C for 1 h. The coating, drying and firing processes were repeated twice. The coating thickness was around 200 nm as measured by optical (interferometric) surface imaging using a WYKO NT-2000 instrument. Additionally, some powders were prepared with a firing temperature of 500–700 °C for XRD measurement.

Differential thermal analysis (DTA) and thermogravimetry (TG) measurements were performed on gelled powders that were dried from the precursor solution at 80 °C. These were carried out on a Setaram 96 instrument with a heating rate of 10 °C min⁻¹. The powders fired at 500, 600 and 700 °C were characterized with X-ray diffraction (XRD) to identify the suitable temperature for forming perovskite phase. The surface morphologies of coatings were examined by optical microscopy and scanning electron microscopy (SEM).

## 3. Results and discussion

Fig. 1 shows the DTA and TG curves of the gelled powders of SSC sol with and without PEG addition. The DTA curve of the gelled SSC powder without PEG addition shows two small and broad exothermic peaks at around 250 and 320 °C, and was followed by a strong exothermic peak at 480 °C. The two peaks at around 250 and 320 °C are attributed to the decomposition and oxidation of acetate groups [18], which are contained in the chelating agent, 2-ethylacetoacetate. The removal of organic residues and water can be responsible for the DTA peak at 320 °C. The strong exothermic peak at 480 °C is attributed to the crystallization of the perovskite phase. The addition of PEG did not obviously change the peak position for the crystallization of the perovskite phase, but brought an additional peak at around 325 °C, which is related to the decomposition of PEG. The XRD patterns for both SSC powder with and without PEG addition fired at 500–700 °C are similar as shown in Fig. 2. It is found that both kinds of powders fired at 500 °C are amorphous. At 600 °C, only partial peaks of SSC appear in the XRD patterns, which mean that the crystallization to the perovskite phase does not finish completely at this temperature. At 700 °C, it is found that well-crystallized powders were formed. From Fig. 1,
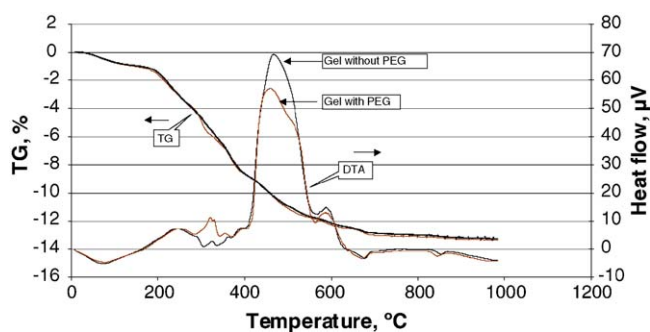


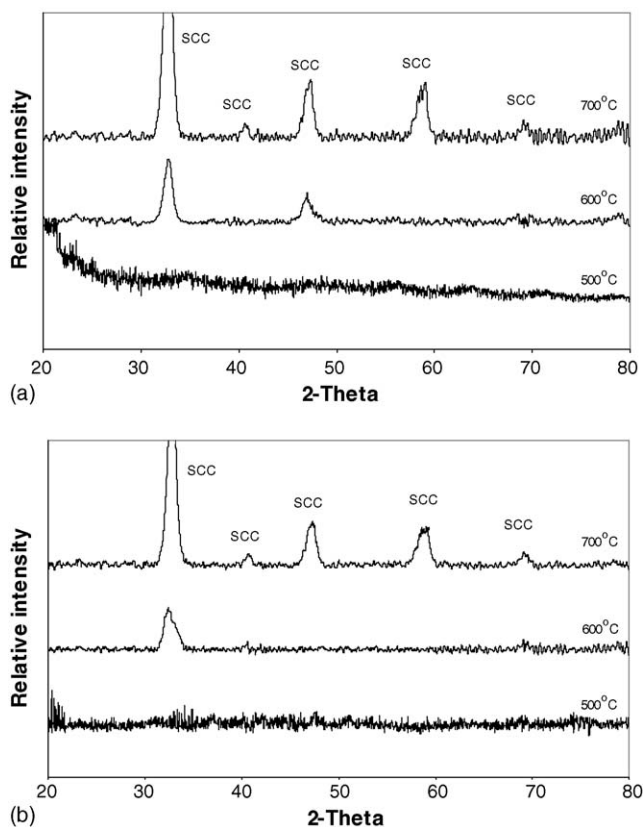Fig. 1. DTA/TG curves of the gelled SSC powders with and without PEG addition.

Fig. 2. XRD patterns of SSC powders sintered at 500, 600 and 700 °C: (a) SSC powders without PEG addition and (b) SSC powders with PEG addition.

the slow TG loss in the temperature range of 400–700 °C indicates that polymeric species still exist in the structure. It is also seen that the XRD pattern at 600 °C show better crystallization for SCC without PEG addition than with PEG addition, which indicated that PEG may retard the SCC crystallization. Based on the above DTA/TG and XRD results, the temperature of 700 °C is identified as optimal for the crystallization of the perovskite phase with or without PEG addition.

Fig. 3 shows the surface morphologies of sol–gel coatings fired at 500, 600 and 700 °C. For the coatings prepared from precursor without PEG addition, amorphous morphologies were observed for those fired at 500 °C. The coating was partially crystallized at 600 °C, and well-crystallized at 700 °C, which is consistent with the XRD results. For the coatings prepared from precursor with PEG addition, quite similar trends were observed, as shown in Fig. 4. However, after firing at 700 °C, the grain size is much finer than that without PEG addition. The grain size for film without PEG addition is around 100 nm, whereas it is only about 50 nm for film with PEG addition.

Polymeric species, such as citric acid, poly(vinyl alcohol), and PEG have been used widely to modify the sols, and subsequently the sol–gel coating microstructures and properties [19–21]. Some researchers have reported acceleration of crystallization in the perovskite-type oxide thin
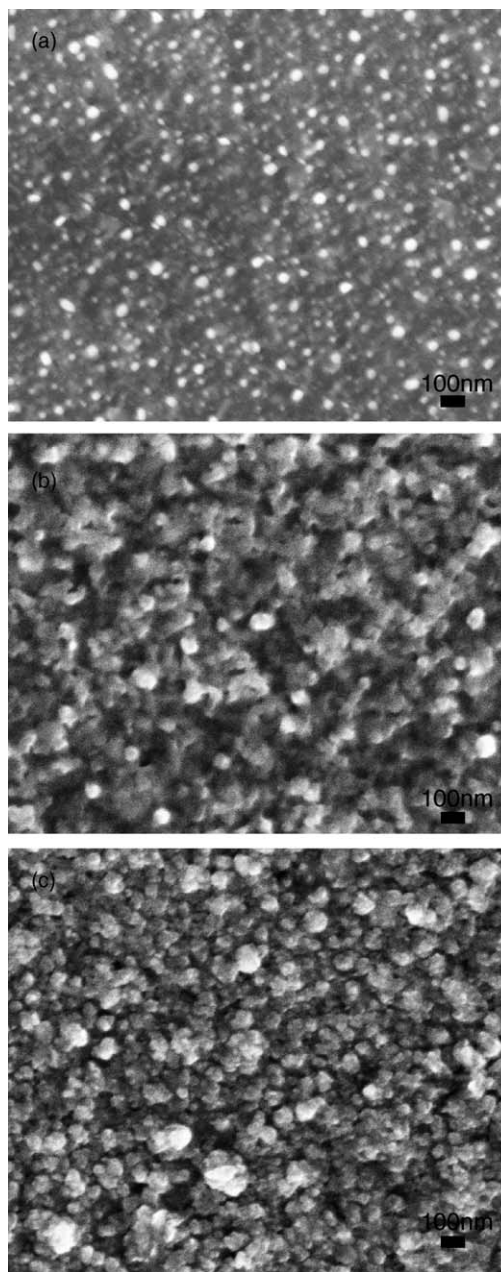


Fig. 3. Surface morphologies of SSC films without PEG addition sintered at: (a) 500 °C, (b) 600 °C and (c) 700 °C.

films or powders prepared from solutions containing the polymeric species, as they can help in the formation of a chelate between constituting cations in the polymer structure. For example, it was reported that PEG assists the crystallization of sol–gel processed LaMnO₃ thin films, and the temperature at which the perovskite phase starts to appear was decreased by 50 °C [19]. However, in other studies, the crystallization was retarded in LaCoO₃ thin films that were prepared from the precursor solution with PEG [20]. In the current study, there was indication that PEG retards the crystallization of the perovskite oxide. In particular, the modification of the precursor solution by PEG refines the grain size of the SSC thin films.
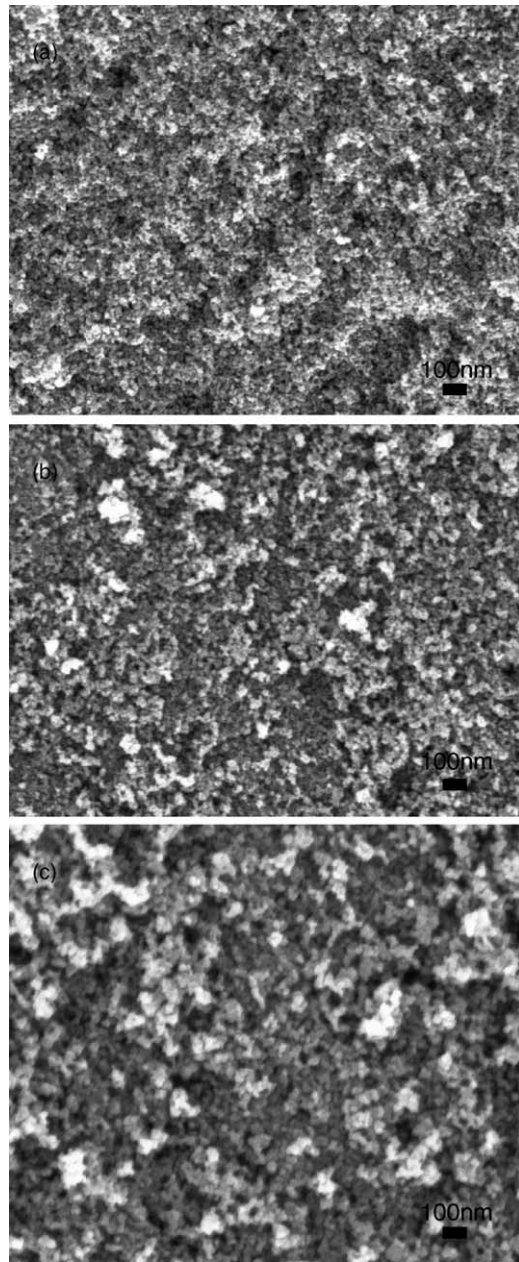
Fig. 4. Surface morphologies of SSC films with PEG addition sintered at: (a) 500 °C, (b) 600 °C and (c) 700 °C.

The different effect of PEG on different perovskite oxides is mostly due to the modification of the network structure of the Sm, Sr–Co precursor solution, according to the particular reaction between $Sm/Sr(O\text{-}i\text{-}C_3H_7)_2$–$Co(CH_3COO)_2$ and PEG. The detailed nature of such modifications to the network structure of the $La(O\text{-}i\text{-}C_3H_7)_2$–$Co(CH_3COO)_2$ precursor solution need further study. The refined SSC film structure should be very beneficial for the SOFC cathode, as its increased surface area should provide more reaction sites for oxygen reduction. For SCC used as cathode, a porous structure is required for gas transportation. One of the advantages of sol–gel process is to easily optimize the porous structure through different parameters, and how to achieve the required porous structure need further study.

## 4. Conclusions

An all-alkoxide route has been developed to prepare sol–gel-derived SSC films on zirconia substrates. XRD, TGA and SEM measurements indicated that single-perovskite phase SSC films were formed when the film was heated at 700 °C. It was found PEG addition slightly retarded the crystallization of SSC perovskite oxide. However, PEG addition significantly refined the crystalline size of SSC film to around 50 nm.

## Acknowledgements

## References

[1] S.C. Singhal, Solid-State Ionics 135 (2000) 305.
[2] R.M. Ormerod, Chem. Soc. Rev. 32 (2003) 17.
[3] B.C.H. Steels, A. Heinzel, Nature 414 (2001) 345.
[4] E. Ivers-Tiffee, A. Weber, D. Herbstritt, J. Eur. Cera. Soc. 21 (2001) 1805.
[5] S. de Souza, S.J. Visco, L.C. De Jonghe, Solid-State Ionics 98 (1997) 57.
[6] Z. Yang, K. Scott Weil, Dean M. Paxton, Jeff W. Stevenson, J. Electrochem. Soc. 150 (2003) A1188.
[7] W.Z. Zhu, S.C. Deevi, Mater. Res. Bull. 38 (2003) 957.
[8] N.Q. Minh, J. Am. Ceram. Soc. 76 (1993) 563.
[9] B.C.H. Steele, Solid-State Ionics 129 (2000) 95.
[10] E. Maguire, B. Gharbage, F.M.B. Marques, J.A. Labrincha, Solid-State Ionics 127 (2000) 329.
[11] V. Dusastre, J.A. Kilner, Solid-State Ionics 126 (1999) 163.
[12] T. Ishihara, M. Honda, T. Shibayama, H. Minami, H. Nishiguchi, Y. Takita, J. Electrochem. Soc. 145 (1998) 3177.
[13] C. Xia, W. Rauch, F. Chen, M. Liu, Solid-State Ionics 149 (2002) 11.
[14] N.Q. Minh, J. Am. Ceram. Soc. 76 (1993) 563.
[15] D. Kuscer, J. Holc, M. Hrovat, S. Bernik, Z. Samardzija, D. Kolar, Solid-State Ionics 78 (1995) 79.
[16] N.Q. Minh, in: S.C. Singhal, M. Dokiya (Eds.), Proceedings of the Sixth International Symposium on Solid Oxide Fuel Cells (SOFC-VI), The Electrochemical Society, Pennington, NJ, 1999, p. 127.
[17] F. Tietz, H.P. Buchkremer, D. Stoever, Solid-State Ionics 152–153 (2002) 373.
[18] S. Bilger, E. Syskakis, A. Naoumidis, H. Nickel, J. Am. Ceram. Soc. 75 (1992) 964.
[19] H.J. Hwang, A. Towata, M. Awano, J. Am. Ceram. Soc. 84 (2001) 2323.
[20] H.J. Hwang, J. Moon, M. Awano, K. Maeda, J. Am. Ceram. Soc. 83 (2000) 2852.
[21] Y. Shimizu, T. Murata, J. Am. Ceram. Soc. 80 (1997) 2702.